Simple lecture demonstrations of instability and self-organization

2014 Phys.-Usp. 57 1130

(http://iopscience.iop.org/1063-7869/57/11/1130)

Physics – Uspekhi **57** (11) 1130 – 1135 (2014)

METHODOLOGICAL NOTES PACS numbers: 01.50.My, **01.55.+b**, **05.65.+b**, 47.20.Bp, 47.20.Ma

Simple lecture demonstrations of instability and self-organization

V V Mayer, E I Varaksina, V A Saranin

DOI: 10.3367/UFNe.0184.201411g.1249

Contents

Abstract. A dielectric liquid layer with an electric field created inside it is proposed as a means for demonstrating the phenomenon of self-organization. The field is produced by the distributed charge transferred by a corona discharge from the tip to the liquid surface. The theory of the phenomenon is presented. An analogy with the Rayleigh–Taylor instability is drawn and a comparison with the Benard instability is given. The practicality of the method for both natural sciences and the humanities is discussed.

1. Introduction

Studying self-organization phenomena in systems of various natures is the subject of the branch of science called synergetics. In physics, the notion of self-organization stands for spontaneous formation of stable patterns in nonequilibrium dissipative systems. The first theoretical studies of synergetic phenomena were carried out nearly half a century ago by I Prigogine and colleagues, and by H Haken directly afterwards. It was found that self-organization takes place in open nonlinear systems at a certain critical value of the external matter or energy flux. The best known and thoroughly studied example of self-organization is offered by the Benard convective hexagonal cells that emerge on heating a horizontal planar layer of fluid from below. Physical phenomena of self-organization also include Faraday ripples, von Kármán vortex streets, Taylor vortices, and the generation of light in a laser.

Current programs in natural sciences always mention the phenomena of instability and self-organization: they are studied in courses of physics [1], and yet they are seldom presented as laboratory experiments. For example, a demonstration of Benard hexagonal cells requires using a setup, albeit simple in its idea, that is rather cumbersome and inconvenient in operation, takes significant time, and does not allow showing the transition from one dissipative structure to another. Offering the possibility of observing the Taylor vortices to the audience requires constructing a special physical setup that is rather complex mechanically [2].

In a lecture, it would be preferable to demonstrate the instability and self-organization phenomena in open systems that do not require special preparation, use ordinary equipment, and occupy a time span of several minutes. This criterion is fully satisfied by the instability of a horizontal layer of viscid fluid on the lower end of a plate and the process of cell pattern formation in a layer of dielectric fluid placed in the field of corona discharge [3].

2. Self-organization in the field of corona discharge

Figure 1 shows a photo of the proposed demonstration setup. A needle, *2*, is placed above a horizontal metal plate, *1*. The plate and the needle are connected to a low-power high-voltage source, *3*. A webcam, *4*, is focused on the plate; its signal after being processed by a computer is sent to the monitor, *5*, and displayed on a large screen with the help of a multimedia projector.

During the demonstration, a drop of transformer or machine oil is dripped on the plate, the needle is adjusted to above the drop center at a distance of several centimeters, and then the voltage between the electrodes is gradually increased. The drop in this case spreads over the plate surface, acquiring the form of a planar layer bound by a cylindrical rim. The rim height is such that the hydrostatic pressure on the fluid in the rim equilibrates the electrostatic pressure in the central drop part. It is known that the electrostatic pressure is caused not so much by an electric wind as by the interaction between the drop surface charged by a corona discharge and the underlying metal plate.

V V Mayer, E I Varaksina, V A Saranin Department of Physics, Korolenko Glazov State Pedagogical Institute, ul. Pervomaiskaya 25, 427621 Glazov, Udmurtskaya Respublika, Russian Federation
E-mail: mvv2011@list.ru, saranin@ggpi.org

Received 5 March 2014
Uspekhi Fizicheskikh Nauk **184** (11) 1249 – 1254 (2014)
DOI: 10.3367/UFNr.0184.201411g.1249
Translated by S D Danilov; edited by A M Semikhatov

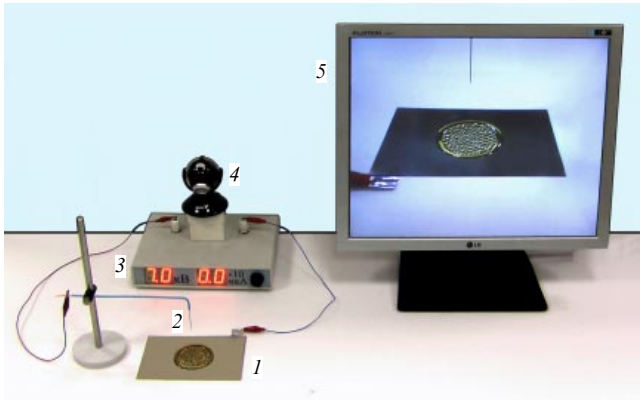

Figure 1. Experimental setup to demonstrate self-organization in a corona discharge field: *1* — metal plate, *2* — needle, *3* — high-voltage source, *4* — webcam, *5* — computer monitor.

Figure 2. A drop of oil in the field of corona discharge.

At a certain voltage, the fluid surface abruptly loses its stability, giving birth to perturbations well seen in reflected light. A further increase in the voltage leads to the onset of an ordered pattern composed of cells of a roughly regular shape. For a given voltage, full equilibration of the ordered structure takes a certain time. It is possible that full equilibration of the cells does not happen for any voltage. A further increase in the voltage results in the decrease in the cell size, with cells continuously appearing and disappearing and displaying a particular structure at any given time moment. If the experiment is realized with a drop of transformer oil 2 mm in thickness and a steel sewing needle with a tip having the curvature radius 0.05 mm, placed 50 mm apart from the drop, the oil surface loses stability at a voltage of approximately 6 kV, while for 20 kV a vigorous process of the appearance and disappearance of small cells can be observed. Figure 2 presents a photo of a typical cell pattern in an oil drop spread in the field of corona discharge.

The phenomenon is apparently explained by the fact that in the corona discharge, ions of the corresponding sign precipitate in the drop surface from the needle tip, creating a charge with a certain density on the surface. Inside the drop, a vertically directed electric field $\mathbf{E}$ is generated. This field creates the electrostatic pressure $p_e = \varepsilon_0 \varepsilon E^2/2$ in the fluid, in addition to the hydrostatic and capillary pressure, causing the instability of the oil surface and the generation of regularly placed cells. Thus, in this experiment, the development of instability leads to self-organization in a fluid layer.

3. Instability of a fluid layer in an electric field

To determine the instability threshold of a gravity–capillary wave in an electric field, we need to derive a dispersion relation that connects the wave increment α with the wave number k. There are different ways of deriving it [4]. In our opinion, the method of deriving the dispersion relation for gravity–capillary waves outlined in Ref. [5] is the simplest and most obvious. We follow it.

Let a planar layer of a fluid with density ρ and thickness h reside on a horizontal, infinitely stretching electrode. We introduce a Cartesian coordinate system with the z axis directed vertically down and the plane $z = 0$ coincident with the equilibrium fluid surface (Fig. 3). We assume the electric field to be confined to the fluid, to be homogeneous, and to be directed along the z axis; we let $\mathbf{E}_0$ denote its field strength.

The equilibrium pressure inside the fluid is the sum of the surface pressure and the hydrostatic pressure,

$$p_r = p_a + \rho g z \,. \tag{1}$$

If there is a small surface perturbation

$$z = \xi(t, x) = \xi_1(t) \exp(-\mathrm{i}kx) \,, \tag{2}$$

the motion of an ideal fluid can be considered to be potential and described by the linearized Euler equation

$$\rho \frac{\partial \mathbf{v}}{\partial t} = -\nabla p \,, \tag{3}$$

where $|p| \ll p_r$ is the pressure perturbation inside the fluid. Using the continuity equation $\operatorname{div} \mathbf{v} = 0$, for the velocity potential Φ in the expression $\mathbf{v} = \nabla\Phi$, we derive the Laplace equation

$$\Delta\Phi = 0 \,. \tag{4}$$

Expressing $\mathbf{v}$ in Eqn (3) in terms of Φ, we obtain

$$\nabla\left(\rho \frac{\partial \Phi}{\partial t} + p\right) = 0 \,. \tag{5}$$

The expression in parentheses can be a function of time, which we set equal to zero [5, p. 36]:

$$\rho \frac{\partial \Phi}{\partial t} + p = 0 \,. \tag{6}$$

For a small perturbation ξ, the pressure perturbation on the surface is composed of hydrostatic and hydrodynamic components, $p = \rho g \xi + p_g$, and it therefore follows from

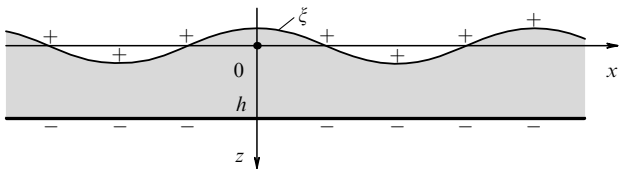

Figure 3. Concerning the theory of the liquid interface instability in an electric field.

Eqn (6) that

$$p_{\mathrm{g}} = -\rho g\xi - \rho\left(\frac{\partial \Phi}{\partial t}\right)_{z=0}. \tag{7}$$

On the other hand, in the presence of an electric field, the pressure in the vicinity of the surface takes the form [6, p. 94]

$$P = p_{\mathrm{a}} + \frac{\rho\varepsilon_0 E^2}{2}\,\frac{\partial\varepsilon}{\partial\rho} + \frac{\varepsilon_0\varepsilon}{2}\,(E_{\mathrm{n}}^2 - E_{\tau}^2)\,. \tag{8}$$

By virtue of the fluid incompressibility and the constancy of the electric field, we can neglect the striction term [7, p. 140]. Using the known relation

$$\int_V \mathrm{rot}\,\mathbf{E}\,\mathrm{d}V = \oint_S (\mathbf{n}\times\mathbf{E})\,\mathrm{d}S\,,$$

the derivation of which is given, for example, in Ref. [8, p. 589], we have the boundary condition

$$(\mathbf{n}\times\mathbf{E})_{z=\xi} = 0 \tag{9}$$

on the fluid surface. It implies the absence of tangential components of the field, $E_\tau = 0$; hence, Eqn (8) gives

$$P = p_{\mathrm{a}} + \frac{\varepsilon_0\varepsilon}{2}\,E_{\mathrm{n}}^2\,.$$

If a perturbation occurs on the fluid surface, the electric field can be written as

$$\mathbf{E} = \mathbf{E}_0 - \nabla\varphi\,, \qquad \Delta\varphi = 0\,, \tag{10}$$

where φ is the potential of the field perturbation. According to the preceding formula, the electrostatic pressure on the surface is expressed as

$$P = p_{\mathrm{a}} + \frac{\varepsilon_0\varepsilon}{2}\,\left[(\mathbf{E}_0 - \nabla\varphi)\mathbf{n}\right]^2,$$

where $\mathbf{n}$ is a unit vector normal to the surface. Hence, up to small first-order terms, we obtain the perturbation of the electrostatic pressure

$$p_{\mathrm{e}} = -\varepsilon_0\varepsilon E_0\left(\frac{\partial\varphi}{\partial z}\right)_{z=0}. \tag{11}$$

The pressure should be balanced on the surface: its hydrodynamic constituent must be equilibrated by the Laplace and electrostatic ones:

$$\begin{aligned} &p_{\mathrm{g}} = p_{\mathrm{e}} + \sigma\left(\frac{1}{R_1} + \frac{1}{R_2}\right)_{z=\xi}, \\ &\frac{1}{R_1} = 0\,, \qquad \left(\frac{1}{R_2}\right)_{z=\xi} = -\frac{\partial^2\xi}{\partial x^2}\,. \end{aligned} \tag{12}$$

From Eqns (7), (11), and (12), we find

$$-\rho g\xi - \rho\left(\frac{\partial\Phi}{\partial t}\right)_{z=0} = -\varepsilon_0\varepsilon E_0\left(\frac{\partial\varphi}{\partial z}\right)_{z=0} - \sigma\,\frac{\partial^2\xi}{\partial x^2}\,. \tag{13}$$

Solutions of Laplace equation (4) for Φ and φ that are periodic in x and satisfy the boundary conditions $\varphi(z)_{z=h} = 0$, $(\partial\Phi/\partial z)_{z=h} = 0$ at $z = h$ have the form

$$\begin{aligned} &\Phi = C_1(t)\cosh\left[k(z-h)\right]\exp\left(-\mathrm{i}kx\right), \\ &\varphi = C_2(t)\sinh\left[k(z-h)\right]\exp\left(-\mathrm{i}kx\right). \end{aligned} \tag{14}$$

To determine $C_2(t)$, we use boundary condition (9). According to Ref. [9, pp. 406, 407], the normal to the perturbed surface can be written as

$$\mathbf{n} = \frac{-\mathbf{i}\xi_x' + 0\mathbf{j} + \mathbf{k}}{\sqrt{1+\xi_x'^2}}\,.$$

Inserting this expression into Eqn (9) and taking (10) into account, we have

$$-\left(\frac{\partial\varphi}{\partial x}\right)_{z=0} + \xi_x' E_0 = 0\,, \tag{15}$$

where the prime denotes the derivative with respect to x. As follows from Eqns (2), (14), and (15),

$$C_2 = \frac{E_0}{\sinh(kh)}\,\xi_1\,,$$

and hence the electrostatic potential perturbation is

$$\varphi = \frac{\sinh\left[k(z-h)\right]}{\sinh(kh)}\,E_0\xi\,. \tag{16}$$

For the velocity potential, we have the kinematic boundary condition

$$v_z = \left(\frac{\partial\Phi}{\partial z}\right)_{z=0} = \frac{\partial\xi}{\partial t}\,. \tag{17}$$

Using Eqn (17), we reduce Eqn (13) to the form

$$\rho g\xi + \rho\,\frac{\partial\Phi}{\partial t} = \varepsilon_0\varepsilon E_0^2\coth(kh)\,k\xi - \sigma k^2\xi\,. \tag{18}$$

We differentiate Eqn (18) with respect to time and recall Eqn (17) to obtain

$$\rho g\,\frac{\partial\Phi}{\partial z} + \rho\,\frac{\partial^2\Phi}{\partial t^2} + \sigma k^2\,\frac{\partial\Phi}{\partial z} - k\varepsilon_0\varepsilon E_0^2\coth(kh)\,\frac{\partial\Phi}{\partial z} = 0\,. \tag{19}$$

Setting $C_1(t) = \exp(\alpha t)$, we obtain from Eqns (14) and (19) that

$$\begin{aligned} \rho g k\sinh(kh) + \rho\alpha^2\cosh(kh) + \sigma k^3\sinh(kh) \\ - k^2\varepsilon_0\varepsilon E_0^2\coth(kh) = 0\,. \end{aligned}$$

Hence follows the dispersion equation

$$\rho\alpha^2 = \left[k^2\varepsilon_0\varepsilon E_0^2\coth(kh) - \rho g k - \sigma k^3\right]\tanh(kh)\,. \tag{20}$$

The instability occurs under the condition $\alpha^2 > 0$; the critical field is determined from the condition $\alpha^2 = 0$ or

$$\varepsilon_0\varepsilon E_0^2 = \left(\frac{\rho g}{k} + \sigma k\right)\tanh(kh)\,. \tag{21}$$

In what follows, it is convenient to take the unit length as the fluid capillary constant $a = \sqrt{\sigma/\rho g}$. Equation (21) can then

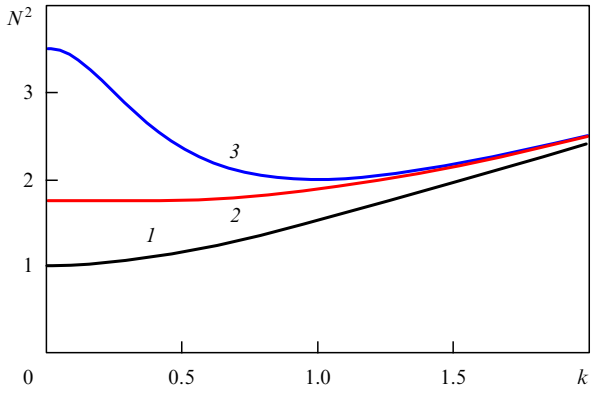

Figure 4. Dependence $N^2(k)$ for different h: *1* — $h = 1$, *2* — $h = \sqrt{3}$, *3* — $h = 3.5$.

be rewritten as

$$N^2 = \frac{\varepsilon_0 \varepsilon E_0^2}{\rho g a} = \left(\frac{1}{k} + k\right) \tanh(kh) . \qquad (22)$$

The dependence $N^2(k)$ for different h is given in Fig. 4. From the plot, it is seen that from the standpoint of instability onset, the most dangerous perturbations for $h = 1$ are long-wave ones, $k = 0$, whereas for $h = 3.5$, these are perturbations with the wave number $k_m \approx 1$. It can be shown [4] that the local minimum on the curve $N^2(k)$ disappears for $h_* = \sqrt{3}a$.

Hence, for $h > h_*$ (h is in units of a), we obtain $k_m \approx 1$ and $N^2 = 2 \tanh h$. Because we already have $\tanh h = 0.964$ at $h = 2$, we can assume that $N^2 \approx 2$ for $h > h_*$. For thin fluid layers, $h < h_*$, we have the asymptotic behavior $k_m \to 0$ and $N^2 = h$. In dimensional form, it gives $\varepsilon_0 \varepsilon E_{0m}^2 = \rho g h$. In that case, for the difference in potentials between the charged surface of the oil layer ($\rho = 0.88 \times 10^3$ kg m^{-3}, $\varepsilon = 2.3$) and the electrode carrying this layer, we obtain

$$U_{0m}^2 = \frac{\rho g}{\varepsilon_0 \varepsilon} h^3 \approx 0.42 h^3 . \qquad (23)$$

4. Experimental substantiation of the theoretical model

Semiquantitative substantiation of the theory presented above can be obtained in a model experiment using a cylindrical container of small diameter with a metal bottom and dielectric walls. Figure 5 presents a series of four photos of the cell structure in the oil layer seen under a sequential increase in the potential difference between the discharging needle tip and the metallic container bottom. It is clearly seen that the phenomenon has a wave origin. By the volume of oil poured into the container, we can estimate the layer thickness and then, for each thickness h, determine the critical voltage U_{0m} at which the surface loses its stability.

Figure 6 plots dependence (23), $U_{0m}^2 = 0.42h^3$ (the straight line) and the experimentally retrieved points in logarithmic axes. We can see encouraging agreement between the experiment and the theory.

5. Analogy with the Rayleigh–Taylor instability

Very roughly, the phenomenon described here can be considered an electric analog of the Rayleigh–Taylor instability. As is known, this type of instability unfolds if a lighter fluid underlies a denser, but immiscible one. In that case, any perturbation leads to oscillations of the flat interface between these fluids. If the length λ of a standing wave excited on this interface exceeds a certain critical value λ_*, the system becomes unstable, and the denser fluid at the top sinks into the troughs of the wave.

In order to create conditions leading to the Rayleigh–Taylor instability, it suffices to switch off the high voltage source in the setup shown in Fig. 1 and turn over the plate with the oil layer on it. In the absence of voltage, the electric field $E_0 = 0$, and from Eqn (20) we find

$$\rho \alpha^2 = -(\rho g k + \sigma k^3) \tanh(kh) . \qquad (24)$$

For the plate with oil turned upside down, we can assume that there is a dense fluid above the lighter one with a negligibly

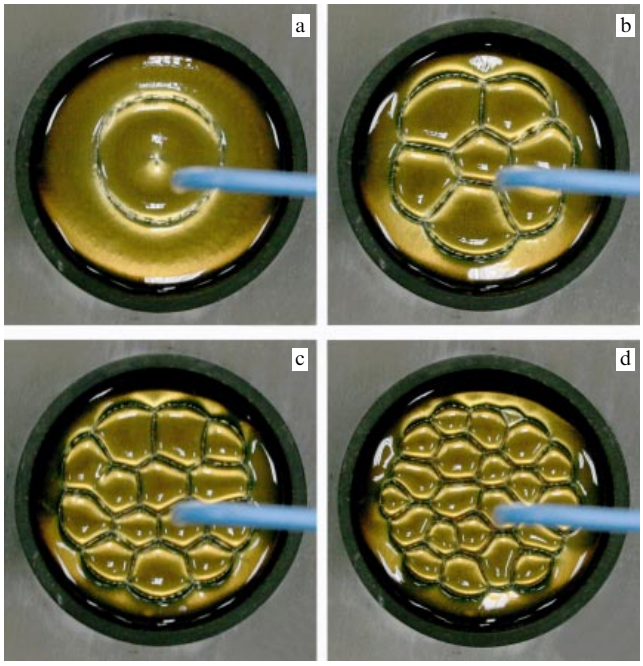

Figure 5. Cell structure in the oil layer upon subsequent increase in the potential difference between the needle in the corona discharge and the metal container bottom for the potential difference of (a) 4.8 kV, (b) 7.7 kV, (c) 9.3 kV, and (d) 11 kV.

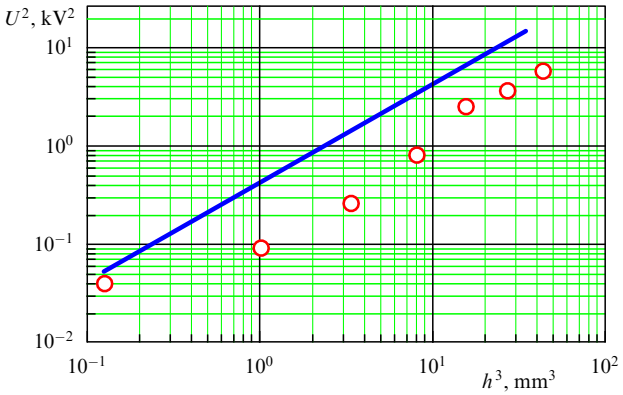

Figure 6. Dependence $U_{0m}^2 = 0.42h^3$ (straight line) and the experimental points in logarithmic axes.

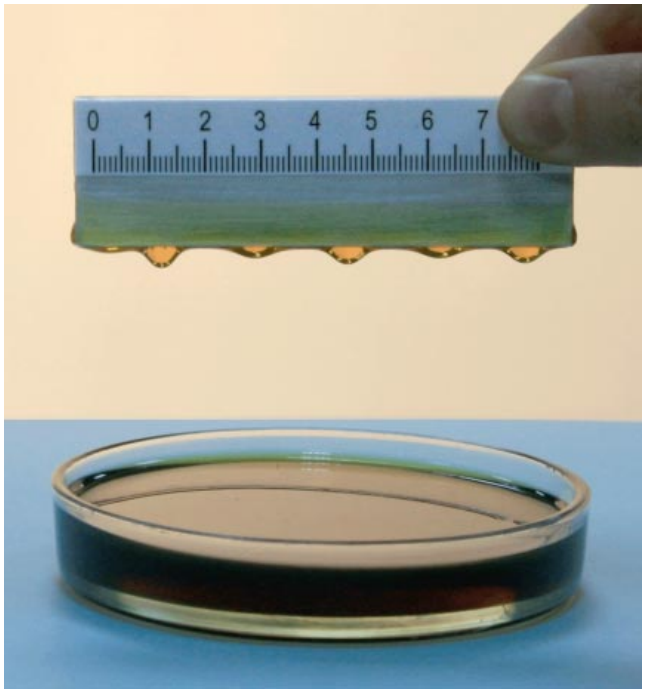

Figure 7. Formation of a gravity–capillary wave on the oil layer (Rayleigh–Taylor instability).

small density. To take this into account, it suffices to reverse the sign of g in Eqn (24).

In that case, all perturbations satisfying the condition

$$k^2 < \frac{\rho g}{\sigma}, \quad \text{or} \quad \lambda > \lambda_* = 2\pi\sqrt{\frac{\sigma}{\rho g}}, \tag{25}$$

exponentially grow as a consequence of the Rayleigh–Taylor instability. The extremum analysis of (24) with the sign of g changed in the limit $kh \to \infty$ indicates that the fastest growth is observed for perturbations of the wavelength

$$\lambda = \lambda_{**} = 2\pi\sqrt{\frac{3\sigma}{\rho g}}. \tag{26}$$

Eventually, just these perturbations lead to the formation of the periodic pattern shown in Fig. 7.

It is not difficult to demonstrate the Rayleigh–Taylor instability in a simple experiment. One fills a shallow container with a sufficiently viscous machine or transformer oil, immerses the edge of a vertical metal plate approximately 5 mm in thickness into the oil, and then takes it out, keeping it over the container. The oil flowing down over the plate forms a layer on its lower edge, whose surface is unstable. As a result, a gravity–capillary wave appears and grows on the surface (see Fig. 7), its crests transforming into drops, which then detach from the plate.

The length λ_{**} of the evolving wave can be measured with a ruler to confirm the validity of expression (26) directly during a lecture.

Returning to the phenomenon of instability of the oil surface in the field of corona discharge, we can draw attention to the analogy between the electrostatic pressure on the oil surface and the hydrostatic pressure of a denser fluid above it. In both cases, the external pressure on the layer surface leads to pattern formation in the layer, which presents an example of self-organization. However, there is an energy flux from outside in the first open system, but a flux of substance in the second.

We note that gravity–capillary waves are studied in all courses of theoretical physics [5], and even if the Rayleigh–Taylor instability is not explicitly mentioned there, the corresponding dispersion relation (24) is derived. Contemporary textbooks [10, 11] present the linear theory of Rayleigh–Taylor instability at the interface of immiscible fluids in sufficient detail.

6. Comparison with the Benard phenomenon

One of the tasks pursued in lecture demonstrations is to form a sensible idea of the physical phenomenon being studied. That is why there is a firm basis for setting up experiments such that the same experimental setup enables visually comparing two physical phenomena whose similarity is revealed by theory.

A comparative demonstration of the instability of a fluid layer in an electric field and under thermal forcing can be readily accomplished if one does not strive to reproduce strictly hexagonal Benard cells. For this, a duralumin container with an internal diameter of 90 mm, wall height of 5 mm, and bottom thickness of 20 mm is placed on an electric heater. The container is filled with transformer oil to form a layer 2–4 mm thick. A discharge needle is placed over the container and the process of cell pattern formation is demonstrated (Fig. 8a, b). Attention is drawn to the confinement of the structure defined by the characteristic geometry of corona discharge.

After that, the heater is switched on, which provides heating of the container bottom, and some powder of aluminum filings is mixed into the oil. With the appearance of convective Benard cells, the heater is turned off and the phenomena taking place in the oil layer are demonstrated (Fig. 8c). The layer thickness can easily be modified by

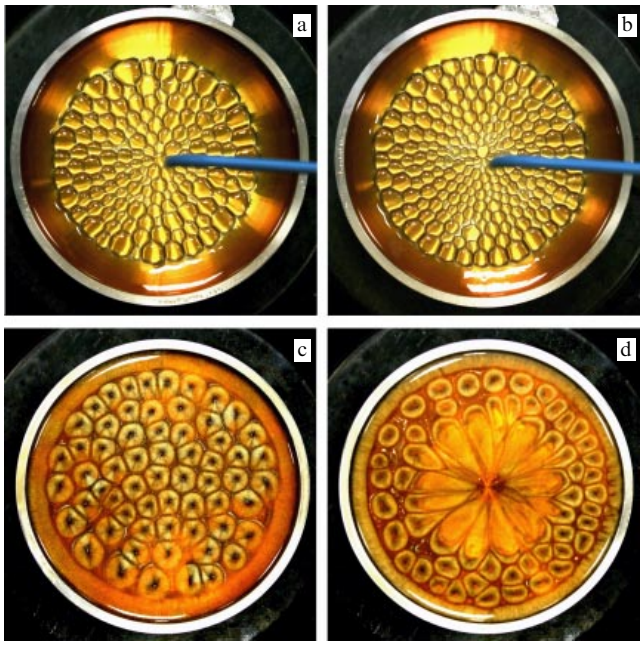

Figure 8. Cell patterns on the oil surface: (a, b) in the field of corona discharge, (c) Benard convective cells, (d) the development of Benard cells on adding a drop of cold oil.

pumping the oil out with a syringe fitted with a silicone tube. Amazingly beautiful dynamically evolving patterns are observed if a drop of cold oil is added to the center of the system of Benard cells (Fig. 8d).

7. Conclusions

The phenomenon of instability of a dielectric fluid layer in the field of corona discharge is notable for the richness of its physical content, the ease of making it available, and the ability to essentially extend the scope of lecture demonstrations of self-organization. The theory of this phenomenon is tightly linked to traditional courses in general and theoretical physics, and can be studied by solving a series of practical exercises. A qualitative explanation of fluid self-organization in an electric field can be taught as an analogy to the Rayleigh–Taylor instability, which provides a possibility of using the phenomenon in question in a broad spectrum of disciplines, both natural sciences and the humanities.

References

1. Belonuchkin V E, Zaikin D A, Tsipenyuk Yu M *Osnovy Fiziki* (Fundamentals of Physics) Vol. 2 *Kvantovaya i Statisticheskaya Fizika* (Quantum and Statistical Physics) (Moscow: Fizmatlit, 2001)
2. Arzhanik A R, Mikhailichenko Yu P *Vestn. Tomsk. Gos. Pedagogich. Univ. Ser. Estestv. Nauki* (2(18)) 85 (2000)
3. Mayer V V, Varaksina E I *Uchebn. Fiz.* (4) 43 (2013)
4. Saranin V A *Ustoychivost' Ravnovesiya, Zaryadka, Konvektsiya i Vzaimodeistvie Zhidkikh Mass v Elektricheskikh Polyakh* (Stability of Equilibrium, Charging, Convection and Interaction of Liquid Masses in Electric Fields) (Moscow–Izhevsk: RKhD, 2009)
5. Landau L D, Lifshitz E M *Fluid Mechanics* (Oxford: Pergamon Press, 1987); Translated from Russian: *Gidrodinamika* (Moscow: Nauka, 1986)
6. Landau L D, Lifshitz E M *Electrodynamics of Continuous Media* (Oxford: Pergamon Press, 1984); Translated from Russian: *Elektrodinamika Sploshnykh Sred* (Moscow: Nauka, 1982)
7. Sivukhin D V *Obshchii Kurs Fiziki* (A General Course in Physics) Vol. 3 *Elektrichestvo* (Electricity) (Moscow: Nauka, 1983)
8. Tamm I E *Fundamentals of the Theory of Electricity* (Moscow: Mir Publ., 1979); Translated from Russian: *Osnovy Teorii Elektrichestva* (Moscow: Nauka, 1976)
9. Bronshtein I N, Semendyayev K A *A Guide Book to Mathematics for Technologists and Engineers* (Oxford: Pergamon Press, 1964); Translated from Russian: *Spravochnik po Matematike dlya Inzhenerov i Uchashchikhsya Vtuzov* (Moscow: Nauka, 1986)
10. Vekshtein G E *Fizika Sploshnykh Sred v Zadachakh* (Physics of Continuous Media in Exercises) (Moscow: Inst. Komp'yut. Issled., 2002)
11. Labuntsov D A, Yagov V V *Mekhanika Dvukhfaznykh Sistem* (Mechanics of Two-Phase Systems) (Moscow: Izd. MEI, 2000)
12. Getling A V *Sov. Phys. Usp.* **34** 737 (1991); *Usp. Fiz. Nauk* **161** (9) 1 (1991)